

Energy analysis of a hybrid parabolic trough collector with a steam power plant in Jordan

Energy Exploration & Exploitation

2023, Vol. 41(6) 1850–1868

© The Author(s) 2023

DOI: 10.1177/01445987231188152

journals.sagepub.com/home/eea



Jamil Al Asfar¹ , Mohammad Alrbai¹
and Nezar Qudah²

Abstract

In this work, a hybrid system consisting of a parabolic trough collector and a steam power plant is proposed. The effect of utilizing the parabolic trough collector on improving the performance of the plant and reducing fuel consumption has been studied experimentally. This study was implemented on a lab scale hybrid energy system consisting of a parabolic trough collector unit incorporated into a biomass-oil shale fired steam power plant during startup conditions. To determine the performance of this lab-scale hybrid system, the efficiency of the parabolic trough collector standalone system has been measured and the flow rate of the system has been tuned to 0.31 L/min to obtain an efficiency of 10.2%. The biomass-oil shale fired power plant worked with superheated steam at 377 °C temperature and 0.6 MPa pressure. The thermal efficiency of the power plant was 12.6% with net output power of 6.3 kW without using the parabolic trough collector unit. It was found that the performance of the hybrid system has shown better efficiency than the standalone biomass fired power plant with the same fuel mixture ratio and steam flowrate. The fuel mixture consumed in the hybrid system decreased by 62.0% at starting up condition. This result may be extended to steady-state operating conditions by increasing the number of parabolic trough collector units utilized. Furthermore, the overall thermal efficiency of the hybrid parabolic trough collector power plant system may reach 33.3% during steady-state operation if 48 parabolic trough collector similar units were used. These parabolic trough collector units should be arranged in three parallel rows, each row of 16 units in series.

Keywords

Oil shale, olive cake, parabolic trough collector, steam power plant, thermal efficiency

¹Mechanical Engineering Department, School of Engineering, The University of Jordan, Amman, Jordan

²Mechanical Engineering Department, School of Engineering Technology, Al Hussein Technical University, Amman, Jordan

Corresponding author:

Jamil Al Asfar, Mechanical Engineering Department, School of Engineering, The University of Jordan, Amman, Jordan.

Email: jasfar@ju.edu.jo



Introduction

Fossil fuels have been the primary source of energy for the world for several decades, but they have several limitations and drawbacks such as their finite resources, environmental impact, geopolitical tensions, price volatility, and health effects (Mohtaram et al., 2022). Based on that, alternative energy sources can be used as a substitute for conventional sources of energy such as fossil fuels (coal, oil, natural gas) that are non-renewable and contribute to climate change effects (Braungardt et al., 2019). Some of the most used alternative energy sources are solar energy, wind energy, hydropower, geothermal energy, and biomass energy (Qazi et al., 2019). Nevertheless, these sources revealed different challenges, such as, their efficiency, storage, working times, and locations. To tackle these issues, hybrid renewable energy systems have been proposed. Biomass is a form of renewable energy that is derived from organic matter, such as plants, crops, and waste materials. Biomass conversion technologies include combustion, gasification, and anaerobic digestion. The use of biomass energy has several advantages as a renewable resource, it is often considered as carbon-neutral since carbon dioxide released during combustion is offset by the carbon dioxide absorbed by the plants during their growth (Xu et al., 2019). The use of hybrid solar-biomass systems uses solar energy and waste biomass to produce electricity, heat, or both. These systems use both renewable resources in a complementary way to increase energy efficiency and reduce greenhouse gas emissions. The basic principle of a hybrid solar-biomass power plant system is to use solar energy to pre-heat up water before entering the boiler (Sobek & Werle, 2019).

An increasing number of countries all over the world have been adopting different approaches to renewable energy sources. As the renewable power technologies are getting better and cheaper, most countries are going with solar, wind, and concentrating solar energy generation (Manasrah et al., 2020).

To avoid these drawbacks, researchers developed biomass-fired power plants to produce clean energy without having to worry about the inconsistencies in the solar and wind energy sources. Biomass-fired power plants can work all year long, day and night, and under different weather conditions. Also, this technology is mature enough to develop different operating conditions and capacities based on the type of biomass and the technology used in burning it. However, their initial cost is relatively high, and the supply chains of biomass are not reliable (Srinivas and Reddy, 2014).

Jordan has been facing real challenges in securing its energy sources due to scarcity of local energy resources and high dependency on imported fuel from neighboring countries, in addition to high continued increase on energy demand for different economic sectors. The significantly high demand was due to the great growth of essential energy demand (about 5.5% annually), and the high increase in electricity generated capacity (7.4% annual) (Abu-Rumman et al., 2020). Jordan is also considered as a hub and transit Arabic state that can play an important role in linking petroleum, gas, and electricity networks through the region. Jordan is constantly dealing with energy shortage threats and there is a serious need for sustainable, renewable energy supplies that will cover the shortage and keep the country in a safe position in this regard (Hamed & Bressler, 2019).

Zhang et al. (2020) performed a study on the thermal optimization of a hybrid renewable energy system that combines solar, hydro, and biomass sources to produce biodiesel in a sustainable and cost-effective manner. The authors used simulation tools to optimize the system's thermal performance, and the results show that the proposed system has a high yield and low cost of biodiesel production, which is also environmentally friendly. The optimized system can also efficiently utilize

the available resources to produce biodiesel, making it a promising option for sustainable energy and biodiesel production. Chen et al. (2021) focused on analyzing a system that combined solar thermal energy and biomass to generate heat and power. They conducted thermodynamic and economic analyses to evaluate the system's efficiency and cost-effectiveness. They found that the solar-aided biomass-fired combined heat and power system was more efficient and had a lower cost of electricity than a standalone biomass-fired system. However, the high initial cost of the solar thermal system could result in a longer payback period. Kumar et al. (2022) aimed to design and optimize a hybrid off-grid power generation system for rural remote electrification in Eastern India using a combination of solar photovoltaic (PV), biomass, diesel, and battery technologies. They conducted a techno-economic analysis to determine the optimal combination of these technologies and found that the hybrid system could provide reliable and affordable electricity to remote communities. The study concluded that the hybrid system can provide a sustainable and cost-effective solution for rural electrification in regions where grid connectivity is limited. Finally, Yahya et al. (2022) examined the performance of a solar-biomass hybrid heat pump batch-type horizontal fluidized bed dryer with a multi-stage heat exchanger for drying paddy. The results show that the dryer achieved a high thermal efficiency and moisture removal rate, with the heat pump and solar collector working together to provide the necessary heat energy. The multi-stage heat exchanger also improved the dryer's performance by increasing the heat transfer efficiency. The study suggests that this type of hybrid dryer can be a viable solution for drying agricultural products in areas with limited access to electricity or conventional fuel sources. Another study by Yashar et al. (2022) focused on investigating a system that combines power generation and cooling using both the ORC and the vapor compression cycle. The results demonstrate that R245fa exhibits the lowest energy destruction rate within the power plant. Additionally, the research indicates that for a turbine inlet temperature of 137 °C, R114 yields the minimum cost function (PCEU), while R142b achieves the minimum PCEU at a turbine inlet pressure of 2500 kPa.

Based on the above discussion, and in order to reduce expenses and generate steam with less biomass products, the hot water produced by the parabolic trough collector (PTC) is interconnected with the biomass boiler to generate steam in this study. Therefore, the objective of present work was to do the following:

- Thermodynamics analysis and experimental testing of a hybrid model of a lab-scale steam power plant involving a constructed 3.6-m length PTC unit was performed. The hybrid system consisted of two main subsystems. The first subsystem is a PTC unit of 3.6-m long, that is utilized for pre-heating the working fluid "water" before entering the boiler of the second subsystem. The second subsystem is a steam power plant that utilizes a mixture of biomass (olive cake) and oil shale as burning fuel.
- This study provides a comprehensive scientific approach to combine a hybrid PTC with a biomass-fired power plant.
- This work addresses technical design guidelines for the optimal combination between PTC and steam power plant to attain the optimum systems performance.

Furthermore, it is expected to solve many problems related to energy and environment issues such as: reducing greenhouse gas emissions, exploiting organic waste from household and agriculture to produce biomass, contributing to Jordanian's energy security, raising the share of renewables in the energy mix and reduce the country's energy bill.

Physical system

A hybrid open-cycle PTC-biomass fired small-scale steam power plant was tested experimentally. The high pressure and temperature steam generated by the boiler expands through a steam turbine coupled with a DC electric generator.

Parabolic trough collector

A 3.6-m long PTC has been constructed. High reflective stainless-steel sheets were used as mirrors in the parabolic trough. A steel structure of 1-m height carries the parabolic trough. The system rotates around its axis to track the sun. A water tank of 1 m³ was installed. A network of pipes is utilized to connect the water tank to the PTC. A water pump of 0.75-HP was used to pump water through the PTC before entering the boiler. A throttle valve was installed after the pump. Figure 1 shows the PTC, while Table 1 shows the full specification of the constructed PTC unit.

The PTC as known, converts received sun radiation into thermal energy used to heat the working fluid/water that circulates in the solar field. The working fluid is pumped from water tank to PTC. The solar field in front of the PTC has copper tubes covered with 3-inch black seamless iron pipes to carry the thermal working fluid. Figure 2 shows these tubes whose length has been increased using loops to enhance the amount of heat transfer process.

Water enters the solar field from the middle of the PTC system flows to the far-left end of the PTC and loops to the far-right end. Finally, it flows out from the middle of the system. This loop allows the water to flow in a solar field of length of 7.2 m. The PTC is equipped with two k-type thermocouples sensors to measure the water temperature before entering the solar field and after leaving the PTC. The water that flows out of the PTC is fed into the second part of the system. Figure 3 shows the implemented PTC system.

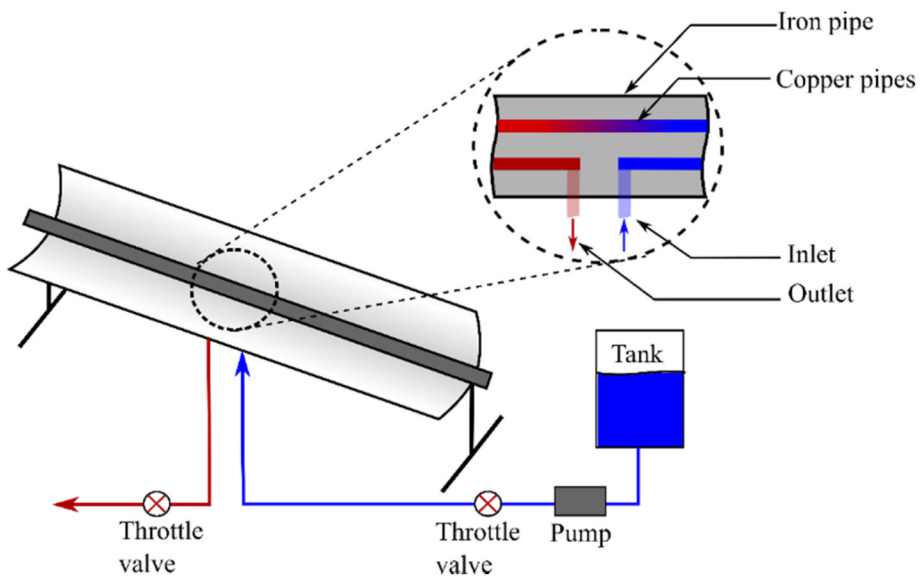


Figure 1. The PTC unit.

Table I. PTC specifications.

| Parameter | Value |
|-----------------------------|-------------------------------------|
| Collector rim angle | 100 degree |
| Reflector surface | Stainless steel sheet |
| Receiver material | Steel |
| Collector aperture | 6.012 m ² (3.6 × 1.67) m |
| Receiver surface treatment | Selective coating |
| Absorber outside diameter | 3 inches |
| Tracking mechanism accuracy | 0.05 |
| Collector orientation | Axis in E-W direction |
| Mode of tracking | N-S tracking |

**Figure 2.** The PTC tubes.

Steam power plant

This part of the system consists of four parts: boiler, fluidized bed burner, piping network, and steam turbine coupled with a generator. Figure 4 shows the whole biomass power plant with all its parts.

Boiler. As in the PTC that conveys thermal energy to water flow inside the pipe, the heat exchanger (boiler) in the biomass-fired plant utilizes heat of combustion from the burned olive cake-oil shale mixture. This heat exchanger is composed of a 34 turn's helical-coil carbon steel. The diameter of these turns is 90.0 cm, and the diameter of the used pipe was 3.8 cm, while the height of this heat exchanger is 4 m. This heat exchanger was installed inside the burner with one of its ends near the



Figure 3. The constructed PTC system.

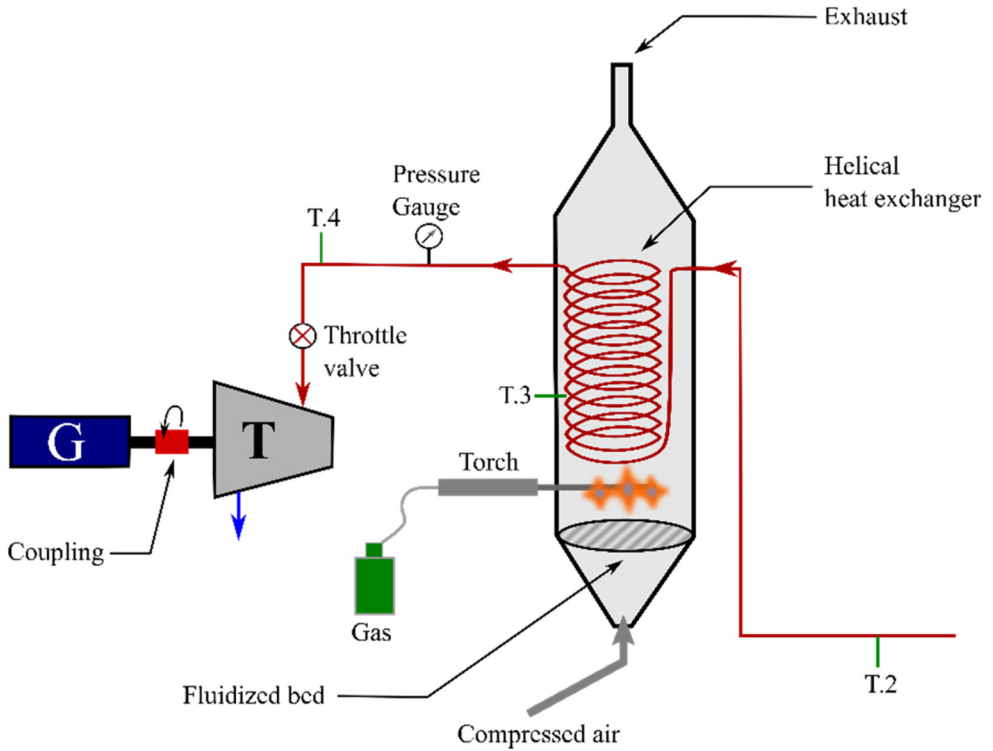


Figure 4. Steam power plant.

highest temperature of the burned mixture. The generated steam powers a steam turbine coupled with a DC generator.

Fluidized bed burner. To speed up the combustion of the mixture, a circulating fluidized bed is utilized. This phenomenon occurs when air that enters through the bed holes from air compressor passes through the mixture's particles. In this case, the fluidized bed converts the solid fuel particles into a dynamic fluid rather than static solid mixture. A fast combustion occurs since the bed increases the surface area of the burned fuel. The fluidized bed is installed under the heat exchanger. To burn the fuel, the compressor inserts air between the fuel particles through the bed and an external LPG gas-torch is used to start the combustion process as shown in Figure 5.

Piping network. The piping network consists of valves, pipes, and a water pump. The water pump is inserted after the water tank and it pumps water into the pipes of the PTC receiver. Subsequently, water stream flows out of the PTC to the heat exchanger as shown in Figure 6.

Steam turbine and generator. An old lab-scale steam turbine manufactured by COPPUS Company (1973) was used. This turbine has the following parameters: maximum number of revolutions of 3000 RPM, counterclockwise rotation with a maximum power of 7.5 kW, turbine efficiency of 80.0%. The turbine is coupled with an electric DC generator of a maximum output power 6.4 kW, separately exited type. Figure 7 shows the used steam turbine and generator.



Figure 5. The biomass-oil shale burner.



Figure 6. Piping network.



Figure 7. The coupled steam turbine and generator.

The complete hybrid system

Figure 8 shows the combination process of PTC and the biomass power plant. This steam plant open cycle starts by pumping the water from the water tank shown in the right in Figure 8. Pumped water flows into the pipes and enters the PTC receiver using shielded pipes. Pumped water continues its cycle in this loop of pipes until it reaches the required temperature. A throttle

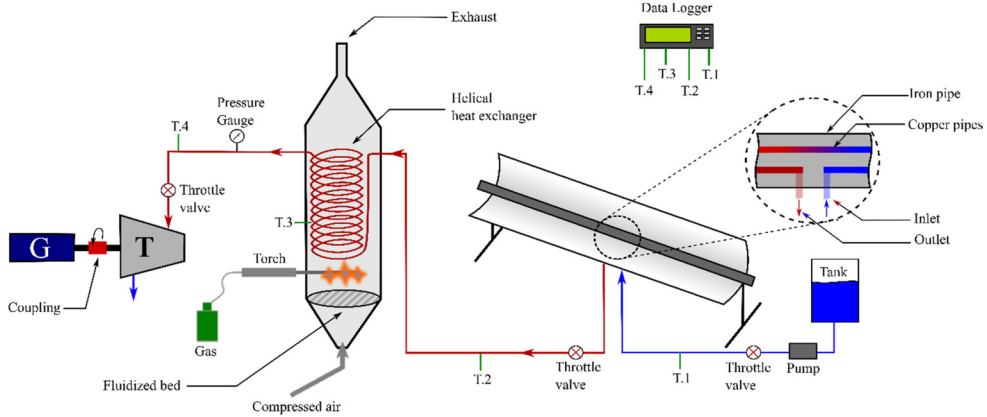


Figure 8. Open cycle hybrid PTC/steam power plant.

valve was installed in the pipes network just before the PTC subsystem, and after it. The first valve controls the flow rate of water in the pipes manually, while the second valve is used to close the boiler after the fluid filling process ends. After the PTC, water enters the heat exchanger (boiler) of the biomass system. When the boiler is filled with heated water, the second throttle valve is closed and the combustion chamber, under the boiler in the figure, is filled with the fuel mixture. Steam is obtained with high pressure and temperature. A third throttle valve is installed on the output pipe to allow steam to flow if its pressure reaches a threshold value, 6 bar in this study. Then, DC electricity is generated as steam flows into the turbine. At the same time, the second throttle valve opens to allow more water to flow inside the boiler.

To measure the performance of the proposed hybrid system, the biomass power plant designed by Al Asfar et al. (2020) has been utilized for comparison. Subsequently, the biomass power plant is redesigned with the PTC part as an initial stage. The performance metric leveraged to compare the performance of these two systems consists of three main parameters as follows:

- The amount of the fuel mixture that has been burned to reach the threshold steam pressure in the boiler.
- The time required to reach the required steam pressure to rotate the turbine.
- The rotational duration of the steam turbine generates the electricity.

Three main scenarios have been configured for the experiment. In all the scenarios, the fuel of the system consisted of a certain amount of mixture of oil shale and olive cake. However, the percentages of these components in the mixture vary. Table 2 shows these mixtures.

Water has been used as the working fluid in the system. The temperature of water inside the initial tank was 20.0 °C. For the first system “the steam plant,” water filled the boiler. The mass flowrate of fuel mixture burning in the fluidized bed burner was 10.56 kg/h, while the mass flowrate of air (oxidizer) was 73.9 kg/h. The air/fuel ratio was around 7/1, while the mass flowrate of steam was 43.2 kg/h. The heating value of the fuel mixture was 17000.0 kJ/kg. In the second system, water flowed to the PTC system before entering the biomass plant to reach a temperature of 45.0 °C. The water flow rate has been tuned using the first throttle valve to allow the water coming out of the PTC system to reach 45.0 °C. This number has been reached with a water flow rate of

Table 2. Mixtures percentages in each scenario.

| Scenario | Olive cake | Oil shale |
|----------|------------|-----------|
| First | 80% | 20% |
| Second | 50% | 50% |
| Third | 30% | 70% |

0.31 L/min. The throttle valve leveraged to control the water flow in this system is a manual valve. Moreover, no water flow rate meter has been used. To overcome this issue, a stopwatch timer and a bottle have been used to measure the rate when 45.0 °C is reached at water exit of the PTC unit.

Mathematical model

The mathematical model representing the governing equations of continuity, energy, mass diffusion, and chemical combustion reactions kinetics during fuel combustion is presented hereunder. These equations were solved using finite-volume method through Fluent/Ansys software, based on a two-dimensional numerical mathematical model. The governing equations including reactions were solved using a high-resolution mesh accounting for the solid and gaseous phases. The k-ε model was used for turbulence and reacting CFD model with same dimension and material of the experimental combustion burner of this study. The burner mesh was created with two velocity inlet surfaces; one for the air and the other for the fuel, one pressure outlet surface at the exhaust and three walls surfaces for the combustion chamber walls. Non-premixed combustion model was selected since the fuel and the oxidizer enter the chamber in distinct streams (Al Asfar et al., 2020). The continuity equation (mass conservation) for a 2-D flow is:

$$\frac{\partial \rho}{\partial t} + \frac{\partial(\rho v_x)}{\partial x} + \frac{\partial(\rho v_r)}{\partial r} + \frac{\rho v_r}{r} = 0 \quad (1)$$

Since non-adiabatic system is assumed, the solution is required for the modeled transport equation for time average enthalpy:

$$\frac{\partial}{\partial t}(\rho h) + \nabla \cdot (\vec{v} \rho h) = \nabla \cdot \left(\frac{k_t}{c_p} \nabla h \right) + S_h \quad (2)$$

Where S_h accounts for source terms due to radiation, heat transfer to wall boundary, and heat exchange with the second phase, and the total enthalpy is defined as:

$$h = \sum_j Y_j h_j \quad (3)$$

Where Y_j is the mass fraction of species j , and

$$h_j = \int_{T_{ref,j}}^T c_{p,j} dt + h_j^0(T_{ref,j}) \quad (4)$$

$h_j^0(T_{ref,j})$ is the formation enthalpy of species j at the reference temperature $T_{ref,j}$. The turbulent viscosity is solved using the $k - \varepsilon$ model that considers:

$$\mu_t = \rho C_\mu \frac{k^2}{\varepsilon} \quad (5)$$

Where k and ε are obtained from the transport equations and C_μ is constant.

The mole fraction of oil shale species during the combustion process were estimated using probability density function (PDF) module integrated in Fluent software. Then, a discrete particle model in a 2-D steady-state space is used to solve numerically the governing equations of continuity, energy, and mass diffusion to estimate: species fraction before and throughout combustion, temperature, radiation, convection heat transfer, pressure, density, and so on. The chemical reversible reactions involving those species during combustion were considered. Those species include C, H, N, O, S, C_(s), S_(s), CH₄, H₂, CO, CO₂, N₂, O₂, OH, H₂O, HS, H₂S, SO, SO₂, CS₂, NO, NO₂, and C₂H₆. The chemical reactions involving above species during combustion were activated; since they were built into fluent PDF module.

Results

The data and results of the biomass plant as a stand-alone electricity generator were obtained and the characteristics and efficiency of the PTC were also estimated. Furthermore, the performance parameters of the hybrid PTC-biomass power plant in terms of overall performance and electricity generation were also calculated and compared with simple corresponding Rankins and Carnot cycles. The detailed outcomes of this experimental and theoretical work are presented hereunder.

Stand-alone biomass boiler results

The biomass boiler and the turbine-generator system were used as a stand-alone system to generate electricity. A mixture of oil shale and olive cake at different concentrations was used as the biofuel of the boiler. Several trial experiments were conducted in this part. The obtained results for the 70.0% oil shale, 30.0% olive cake mixture were not acquired since the mixture did not ignite fully with the gas torch. The 50.0% oil shale, 50.0% olive cake mixture also did not ignite, while the 20.0% oil shale, 80.0% olive cake was successfully ignited.

The temperature of steam inside the heat exchanger of the boiler at the outlet point (i.e. T4 in Figure 8) against time are presented in Figure 9. The time taken by steam to reach 377.0 °C and 6 bar was around 140 min as indicated in the figure. The fuel burning rate of the mixture was 10.6 kg/h.

The calorific value of the mixture was also calculated based on the lower heating values (LHV) of the oil shale and olive cake. According to Al Asfar et al. (2020), the calorific values of the oil shale and olive cake are 7000.0 and 19500.0 kJ/kg, respectively. Hence, the calorific value of the mixture is estimated as follows (Moran et al., 2020):

$$C.V_{fuel\ mix} = m_1 \times HV_1 + m_2 \times HV_2$$

$$C.V\ of\ mix = 0.2 \times 7000 + 0.8 \times 19500 = 17000\ kJ / kg$$

Therefore, the output power of the biomass boiler was estimated by multiplying the burning rate of the mixture by its calorific value. It represents the amount of heat that is transferred to working fluid water inside the heat exchanger. Hence, the input power of the turbine is equal to:

$$\text{Input power} = 0.0029 \left[\frac{kg}{s} \right] \times 17000 \left[\frac{kJ}{kg} \right] = 50\ kW$$

Considering that the rated output power of the turbine is 6.3 kW, the overall efficiency of the plant is estimated as follows:

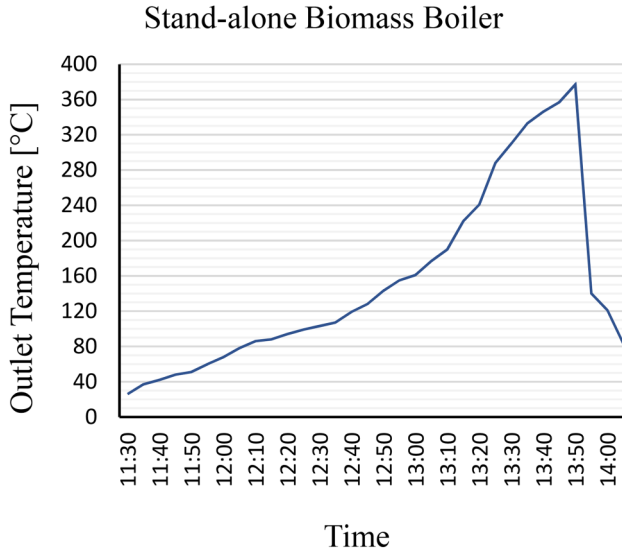


Figure 9. Temperature inside the heat exchanger (the boiler) at the outlet point.

$$\text{Overall efficiency} = \frac{\text{Output}}{\text{Input}} = \frac{6.3 \text{ kW}}{50 \text{ kW}} = 12.6\%$$

As shown from Figure 9, the temperature of steam that entered the turbine was 377 °C. Steam was only released to the turbine when it reached 0.6 MPa of pressure. According to thermodynamics tables, the generated steam was at superheated state (377.0 °C and 0.6 MPa). Therefore, the generated steam had an enthalpy value of 3050.0 kJ/kg and an entropy value of 6.38 kJ/kg.K (Moran et al., 2020).

Stand-alone PTC results

The parabolic solar collector was tested before connecting output hot water to boiler. The first test was conducted by applying 0.51 L/min water flow to the PTC. The second trail was conducted, however, using 0.31 L/min water flow. Figure 10 shows the output temperature of the water against time in both cases. As shown in the figure, the output temperature of water at steady state was 34.0 °C for the 0.51 L/min flow, and 45 °C for the 0.31 L/min flow. The inlet temperature of the water, however, was fixed for both cases at 20.0 °C. Therefore, the amount of heat transferred from the PTC to the water was estimated as follows:

$$\dot{Q}_{0.5L/min} = \dot{m} \times C_p \times \Delta T = \frac{0.51}{60} \times 4.2 \times (34 - 20) = 0.49 \text{ kW}$$

$$\dot{Q}_{0.3L/min} = \dot{m} \times C_p \times \Delta T = \frac{0.31}{60} \times 4.2 \times (45 - 20) = 0.525 \text{ kW}$$

The aperture area of the PTC is calculated as 6.02 m² and the average irradiance from sun was around 850 W/m² during the days of experimental work. Consequently, the efficiency of the PTC was calculated as follows:

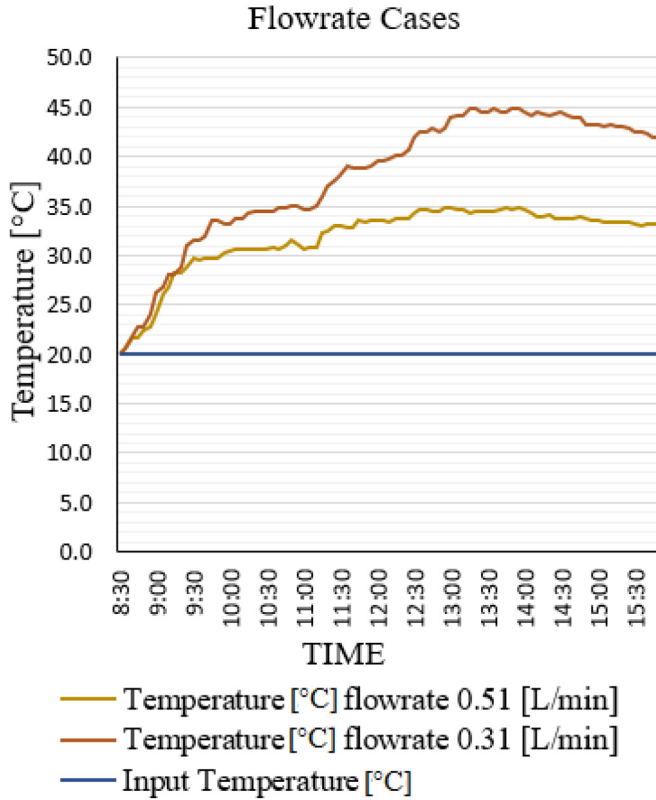


Figure 10. Output temperature of water against time in both flowrate cases.

$$\eta_{0.5L/min} = \frac{\dot{m} \times C_p \times \Delta T}{G \times A} = \frac{0.49 \text{ kW}}{0.850 \left[\frac{\text{kw}}{\text{m}^2} \right] \times 6.02[\text{m}^2]} = 9.5\%$$

$$\eta_{0.3L/min} = \frac{\dot{m} \times C_p \times \Delta T}{G \times A} = \frac{0.525\text{kW}}{0.850 \left[\frac{\text{kw}}{\text{m}^2} \right] \times 6.02[\text{m}^2]} = 10.2\%$$

Hybrid PTC-biomass results

The parabolic solar collector was used to pre-heat the water to 45.0 °C in a 0.31 L/min flow rate. Pre-heated water was used as the input source for the biomass boiler. The results showed that the temperature increments at the output of the heat exchanger inside the boiler reached 377.0 °C at 0.6 MPa. Figure 11 shows the temperature of water inside the exchanger against time.

In this work, the maximum temperature of 377.0 °C and 0.6 MPa was reached in only 61.0 min in starting up condition of the hybrid system, which means that pre-heating water before entering the biomass boiler saved around 80 min of fuel burning time. In other words, similar steam temperature and pressure were reached in the hybrid system 62.0% quicker than the stand-alone

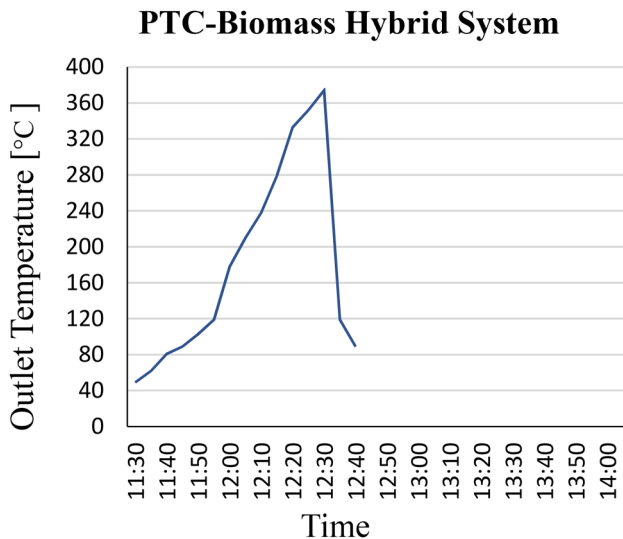


Figure 11. Temperature of water inside the exchanger against time with PTC.

boiler. Furthermore, the same trend is noticed when the pressure valve was released. Figure 11 shows also the significant temperature drop due to the sudden loss of pressure inside the heat exchanger/boiler when steam entered the turbine during the test.

In order to initiate a comparison between the hybrid system and the stand-alone biomass system, the burning rate was the same in both cases at 0.0029 kg/s. Therefore, it can be calculated that only 11.4 kg of biofuel mixture was needed for water to reach a similar state as shown here:

$$\text{Fuel mass} = 0.0029 \left[\frac{\text{kg}}{\text{s}} \right] \times \left(61[\text{min}] \times \frac{60[\text{s}]}{1[\text{min}]} \right) = 11.4 \text{ kg}$$

$$\text{Fuel mass savings} = \frac{(30 - 11.4)}{30} \times 100\% = 62\%$$

Based on the above equation, 62.0% fuel saving was achieved at starting up. Therefore, the overall efficiency of the plant may be estimated as follows.

It is recommended to use 48 PTC similar units arranged in three parallel rows with 16 units in series, in order to get higher thermal efficiency of the conventional power plant system by 20.7%, based on 43.2 kg/h mass flowrate of steam in the boiler and turbine in steady-state operation of this hybrid system:

$$\text{overall efficiency(theoretical)} = \frac{\text{Output}}{\text{Input}} = \frac{6.3 \text{ kW}}{18.9 \text{ kW}} = 33.3\%$$

Consequently, the properties of Rankine cycle of the system (T - s diagram) were represented in Figure 12.

Where:

State 1: $T_1 = 20.0 \text{ }^\circ\text{C}$, $P_1 = 100 \text{ kPa}$, $h_1 = 84 \text{ J/kg}$

State 2: $T_2 = 150.0 \text{ }^\circ\text{C}$, $P_2 = 600 \text{ kPa}$, $h_2 = h_1 + v \Delta P = 84.5 \text{ kJ/kg}$

State 3: $T_3 = 377.0 \text{ }^\circ\text{C}$, $P_3 = 600 \text{ kPa}$, $h_3 = 3200 \text{ kJ/kg}$, $s_3 = 7.6 \text{ kJ/kg.K}$

State 4: $T_{4s} = 150.0 \text{ }^\circ\text{C}$, $T_{4a} = 196 \text{ }^\circ\text{C}$, $P_4 = 100 \text{ kPa}$, $s_4 = s_3 = 7.6 \text{ kJ/kg.K}$

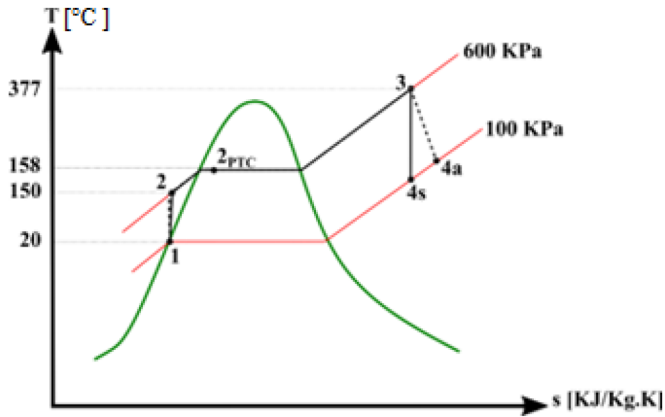


Figure 12. Representation of the open Rankine cycle of the system.

The enthalpy at 4 s is determined from the thermodynamics tables: $h_{4s} = 2776$ kJ/kg.

However, the enthalpy at 4a is determined from the rated turbine efficiency, which is found to be 80% according to its datasheets. The turbine efficiency is estimated as follows ($h_{4a} = 2860.0$ kJ/kg):

$$\text{Turbine efficiency} = \frac{h_3 - h_{4a}}{h_3 - h_{4s}} = 0.8$$

For the hybrid system, the enthalpy at point 2_{PTC} from the figure is estimated assuming the use of 48 PTC units. Therefore, it can be determined that:

$$q_{\text{hybrid}} = q_{\text{boiler}} \times 38 \%$$

Where q_{boiler} is determined from the difference between h_3 and h_2 which equals to 3115.5 kJ/kg. Hence, the enthalpy at 2_{PTC} is determined as follows:

$$q_{\text{hybrid}} = h_3 - h_{2PTC} \rightarrow h_{2PTC} = 1953.8 \text{ kJ/kg}$$

Considering a cycle that includes heat transfer only with a maximum temperature at 377 °C and a low temperature at 20.0 °C as a sink, the maximum efficiency can be calculated as follows:

$$\eta_{th, rev} = 1 - \frac{T_L}{T_H}$$

$$\eta_{th, rev} = 1 - \frac{20 + 273}{377 + 273} = 54.9\%$$

Therefore, the improved overall thermal efficiency of the proposed hybrid steam plant may reach 33.3% if 48 PTC units were used.

Uncertainty analysis

The uncertainty analysis is often used to estimate the accumulative errors in the experimental work. It highlights the differences between the measured and true values in the readings. For each measurement tool, or method, the uncertainty analysis can be calculated via repeated measures or by simply determining the reading error of the tool from the datasheets or by evaluation.

In the experiments, four types of measuring tools and methods were used. A k-type thermocouple to measure the temperature, a luggage weighing scale to measure the weight of the biomass fuel, a container-stopwatch method to measure the flow rate of water, and an analog pressure gauge to measure the pressure of steam. Also, in this study, the uncertainty of the data harvesting unit will be assumed to be zero since there is no direct evidence of the unit's accuracy.

For the k-type thermocouple, the maximum error that may be obtained from a reading is $\pm 0.4\%$. As for the weighing scale, it is estimated that the error is around $\pm 0.1\%$. Also, for the analog pressure gauge, an average error is estimated at $\pm 0.1\%$ (thermocouple accuracy, 2021 and pressure gauge instruments, 2021). However, the error in the flow rate was determined by repeating the timer readings 10 times. The standard deviation of the readings for the 0.31 L/min was ± 0.05 . The following equation was used to determine the overall uncertainty as a combination of all the errors (Holman, 2012):

$$u_c = \sqrt{u_t^2 + u_w^2 + u_p^2 + u_f^2} = 0.42\%$$

Environmental effect

The environment is a priority when studying biomass, as burning biomass contributes to the formation of acid rain and smog, same as fossil fuels. Nitrogen and sulfur dioxide are captured by moisture to form acid rain, which in turn may cause clouding, dry disposition, and severe effects on ecosystems. Figure 13 represents the emitted pollutants due to biomass mixture combustion, estimated through the simulation process done by authors in previous study (AlShawawra and Asfar, 2018). The fluidized bed technology used here is characterized by its easy desulfurization and lower emissions (Akpulat et al., 2010). Besides the low concentrations of sulfur, resulting from olive cake < 0.1 wt % compared to other bio-wastes (Al-Rousan et al., 2013). It is worth noting that the sulfur

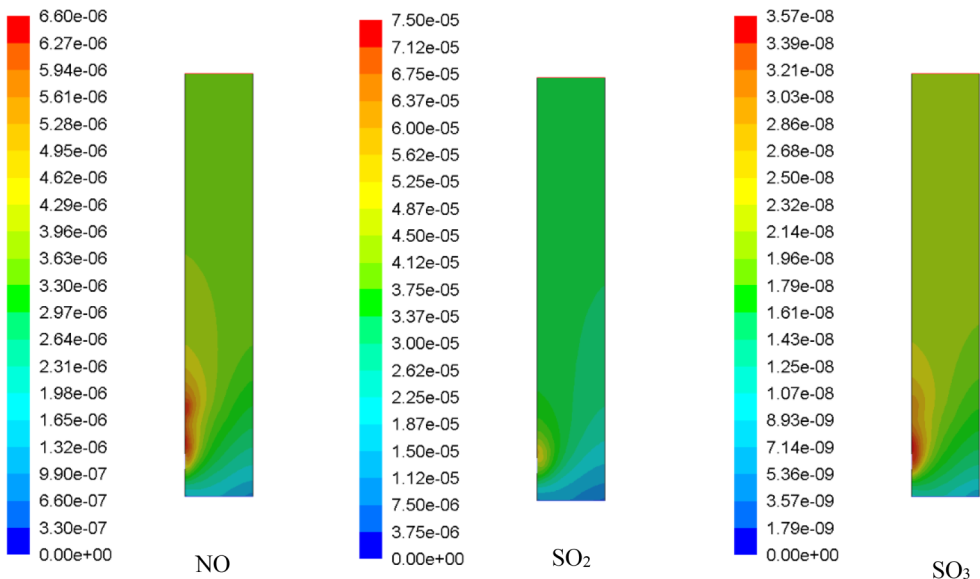


Figure 13. Mass fraction of pollutants for direct burning of biomass mixture.

may be reduced by introducing hydrogen desulfurization technique (Song, 2003). HDS technique is based on using hydrogen to minimize the sulfur concentration. Petracchini et al. (2017) added a desulfurization unit to a prototype plant partially fed by olive cake where they monitored the hydrogen sulfide content and noticed substantial reduction from 95–140 ppm to 4–8 ppm before and after the desulfurization process, respectively.

Cheah et al. (2009) investigated the desulfurization of both biomass and coal derived syngas at mid to high temperature ranges. They stated that biomass feedstock has low percentage of sulfur species and removed these sulfur species before entering the power generation. Sorbents based on zinc, iron, calcium, manganese, and copper have been used to remove H₂S from coal extracted.

Conclusions

In this work, a series of experimental tests were conducted to a stand-alone biomass boiler, a solar power concentrator (in a shape of a parabolic trough), and a hybrid biomass-PTC system. The main objective of these tests was to investigate the effects of the systems' parameters on its performance. These studied parameters included: steam temperature, generated power, and fuel savings in the hybrid system.

- The results of the stand-alone biomass boiler showed that the maximum temperature of steam reached 377 °C at 0.6 MPa. The produced steam was used to generate electricity via a steam turbine coupled with an electric generator.
- The overall efficiency of the turbine reached 12.6% at the rated power output of 6.3 kW. Results were also obtained for the parabolic thermal collector as a stand-alone system. The efficiency of the PTC system at 0.31 L/min was around 10.2%. The water temperature at the outlet of the PTC unit reached 45 °C at steady state for an inlet temperature of 20.0 °C.
- Similar steam temperature was obtained with 62% less in time at startup than the conventional stand-alone biomass plant. This means that 62.0% saving of burned fuel in starting up conditions was achieved.
- The improved overall efficiency of the proposed hybrid steam plant may reach 33.3% if 48 PTC total similar units were used. These units should be arranged in three parallel rows, each of 16 units in series.

Declaration of conflicting interests

The author(s) declared no potential conflicts of interest with respect to the research, authorship, and/or publication of this article.


Funding

The author(s) received no financial support for the research, authorship, and/or publication of this article.

Data Availability

Please note that all materials related to our study (e.g. data, samples, or models) can be accessed easily by any future research articles or work.

ORCID iD

Jamil Al Asfar  <https://orcid.org/0000-0001-5539-7322>

References

- Abu-Rumman G, Khdair AI and Khdair SI (2020) Current status and future investment potential in renewable energy in Jordan: An overview. *Heliyon* 6(2): 1–8.
- Akputat O, Varol M and Atimtay AT (2010) Effect of freeboard extension on co-combustion of coal and Olive Cake in a fluidized bed combustor. *Bioresource Technology* 101(15): 6177–6184.
- Al-Rousan A, et al. (2013) Prospects of synthetic biodiesel production from various bio-wastes in Jordan. *Journal of Sustainable Bioenergy Systems* 03(03): 217–223.
- Al Asfar J, AlShwawra A and Shaban NA (2020) Thermodynamic analysis of a biomass-fired lab-scale power plant. *Energy* 194: 116843.
- AlShwawra A and Asfar JA (2018) Simulation of olive cake combustion in a fluidized bed burner. *International Journal of Mechanical Engineering and Robotics Research* 7(5): 483–488.
- Braungardt S, van den Bergh J and Dunlop T (2019) Fossil fuel divestment and climate change: Reviewing contested arguments. *Energy Research & Social Science* 50: 191–200.
- Cheah S, Carpenter DL and Magrini-Bair KA (2009) Review of mid- to high-temperature sulfur sorbents for desulfurization of biomass- and coal-derived syngas. *Energy & Fuels* 23(11): 5291–5307.
- Chen H, Xue K and Wu Y (2021) Thermodynamic and economic analyses of a solar-aided biomass-fired combined heat and power system. *Energy* 214: 119023.
- Hamed TA and Bressler L (2019) Energy security in Israel and Jordan: The role of renewable energy sources. *Renewable Energy* 135: 378–389.
- Holman JP (2012) *Experimental Methods for Engineers*. Boston: McGraw-Hill/Connect Learn Succeed.
- Kumar P, Pal N and Sharma H (2022) Optimization and techno-economic analysis of a solar photo-voltaic/biomass/diesel/battery hybrid off-grid power generation system for rural remote electrification in eastern India. *Energy* 247: 123560.
- Manasrah A, Alkhalil S and Masoud M (2020) Investigation of multi-way forced convective cooling on the backside of solar panels. *International Journal on Energy Conversion (IRECON)* 8(5): 181.
- Mohtaram S, et al. (2022) Multi-objective evolutionary optimization and thermodynamics performance assessment of a novel time-dependent solar Li-Br absorption refrigeration cycle. *Science China Technological Sciences* 65: 2703–2722.
- Moran MJ, Shapiro HN, Boettner DD, et al. (2020) *Fundamentals of Engineering Thermodynamics*. Ohio, USA: WILEY, Ohio State University.
- Petracchini F, Paolini V and Liotta F (2017) Vacuum swing adsorption on natural zeolites from tuffs in a prototype plant. *Environmental Progress & Sustainable Energy* 36(3): 887–894.
- Qazi A, Hussain F and Rahim NABD (2019) Towards sustainable energy: A systematic review of renewable energy sources, technologies, and public opinions. *IEEE Access* 7: 63837–63851.
- Sobek S and Werle S (2019) Solar pyrolysis of waste biomass: Part 1 reactor design. *Renewable Energy* 143: 1939–1948.
- Song C (2003) An overview of new approaches to deep desulfurization for ultra-clean gasoline, diesel fuel and jet fuel. *Catalysis Today* 86(1–4): 211–263.
- Srinivas T and Reddy BV (2014) Hybrid solar–biomass power plant without energy storage. *Case Studies in Thermal Engineering* 2: 75–81.
- Xu H, Sun XY and Dai YJ (2019) Thermodynamic study on an enhanced humidification-dehumidification solar desalination system with weakly compressed air and internal heat recovery. *Energy Conversion and Management* 181: 68–79.
- Yahya M, Rachman A and Hasibuan R (2022) Performance analysis of solar-biomass hybrid heat pump batch-type horizontal fluidized bed dryer using multi-stage heat exchanger for paddy drying. *Energy* 254: 124294.
- Yashar A, et al. (2022) Energy, exergy and economic analysis of combined solar ORC-VCC power plant. *International Journal of Low-Carbon Technologies* 17: 196–205.
- Zhang X, Yang J and Fan Y (2020) Experimental and analytic study of a hybrid solar/biomass rural heating system. *Energy* 190: 116392.

Appendix

Notation

| | |
|------------------------|--|
| RC | Rankine cycle |
| CO ₂ | carbon dioxide |
| TEGs | thermoelectric generators |
| Bar | the metric unit of pressure |
| PV | photovoltaic |
| C.V | calorific value |
| η | efficiency |
| PTC | parabolic solar collector |
| PTC | concentrated solar power |
| m | mass [kg] |
| A | area [m ²] |
| ρ_{air} | density of air [$\frac{\text{kg}}{\text{m}^3}$] |
| ρ_{solid} | density of solid [$\frac{\text{kg}}{\text{m}^3}$] |
| A | ash |
| VM | volatile material |
| μ | dynamic viscosity [$\frac{\text{N}\cdot\text{s}}{\text{m}^2}$] |
| \dot{m}_{air} | mass flow rate of air [$\frac{\text{kg}}{\text{s}}$] |
| (F/A)stoic | stoichiometric fuel to air ratio [$\frac{\text{kg solid}}{\text{kg air}}$] |
| $(\frac{F}{A})_{act.}$ | actual fuel to air ratio [$\frac{\text{kg solid}}{\text{kg air}}$] |
| \emptyset | equivalence ratio |
| \dot{m}_{solid} | mass flow rate of solid [$\frac{\text{kg}}{\text{s}}$] |
| \dot{V}_{air} | volumetric flow rate of air [$\frac{\text{ft}^3}{\text{min}}$] |
| HHV | higher heating value [$\frac{\text{kJ}}{\text{kg}}$] |
| LHV | lower heating value [$\frac{\text{kJ}}{\text{kg}}$] |
| DAF | dry ash free |
| FC | fixed carbon |